**NURETH14-202** 

### SAFETY ANALYSES FOR A SCWR IN-PILE FUEL ASSEMBLY

M. Raqué<sup>1</sup>, I.Vasari<sup>2</sup> and T. Schulenberg<sup>3</sup>

<sup>1</sup> EnBW Kernkraft GmbH, Germany

<sup>2</sup> TÜV Süd Energietechnik GmbH, Germany

<sup>3</sup> Karlsruhe Institute of Technology, Germany

raque@iket.fzk.de, ivan.vasari@tuev-sued.de, schulenberg@kit.edu

#### **Abstract**

A Supercritical-Water Cooled Reactor (SCWR) test fuel element is intended to be inserted into a research reactor. The test section will be operated at temperatures and pressures above the thermodynamic critical point of water. It contains four fuel rods with a total heating power of 53 kW and it is connected with a 300 °C closed coolant loop, which is equipped with two active safety systems and a depressurization system to cool the fuel rods in case of an accident. The paper explains the physical models for numerical simulations of the safety system. Some accident sequences are analyzed exemplarily to illustrate the system performance.

# 1. Introduction

In the framework of the Generation IV International Forum (GIF) a number of different reactor concepts are being investigated to meet the requirements for future nuclear energy production. One of them is the Supercritical-Water Cooled Reactor (SCWR) concept. From 2006 to 2010, a consortium of 13 partners from 8 Euratom member states has been working on the concept of a 1000 MWe reactor with a thermal core, which they called the High Performance Light Water Reactor (HPLWR) [1]. Aiming at increased thermal efficiencies as compared to conventional light water reactors, the HPLWR shall be operating at temperatures and pressures well above the thermodynamic critical point of water (T = 374 °C, p = 22.1 MPa), yielding supercritical working conditions inherently avoiding safety-related two-phase flow phenomena such as boiling crisis and dryout during normal operation. However, the consequences to be faced are higher material requirements and a significantly higher heat-up of coolant in the core.

As a SCWR has never been built before, the next step after this design study is intended to be an in-pile fuel qualification test in the Czech research reactor LVR-15 at CVR in Řež in order to examine the material and thermal-hydraulic behavior under supercritical water conditions and to develop a licensing process for nuclear facilities with supercritical water, in general. A pressure tube containing 4 fuel rods with UO<sub>2</sub> fuel of up to 20% enrichment shall be inserted into the existing research reactor LVR-15, replacing one of the standard fuel assemblies. The pressure tube is connected with a 300 °C closed coolant loop and a primary pump located outside the reactor building. The fuel rods shall produce a total heating power of 53 kW. A recuperator

inside the pressure tube preheats the coolant to hot channel conditions as they are predicted to occur in the first heat-up step of the three-pass-core design of the HPLWR. Furthermore, this loop contains two active safety systems and a depressurization system to cool the fuel rods in case of an accident. The test section has been described in a pre-conceptual design study by Raqué et al. [2] and the concept of the required safety system has been worked out by Schneider et al. [3] based on numerical simulations with APROS [4].

Parametric CFD analyses of the heated sections [2] showed that a coolant mass flow rate of 0.14 kg/s results in overheated claddings. For steady state operation of the test section, an effective cooling of the rods could only be achieved with an increased mass flow of 0.24 kg/s. On the other hand, Schneider et al. [3] showed with numerous transient simulations that the proposed safety systems of the loop work in principle. As their model did not take into account the density feedback on the heating power of the fuel rods, however, this mechanism was implemented now in the actual model presented in this paper. Moreover, the present model allows to determine the surface temperatures of the fuel rod claddings, as will be described below. In addition, analyses of the initial system configuration [3] indicated temperature peaks during some accident scenarios, which occurred right after depressurization. These peaks could be avoided by optimizing the diameters of the pipes connecting the compensators with the system.

## 2. Design of the test loop and its safety systems

The basic high pressure loop of the fuel qualification test consist of the mentioned test fuel element, which is inserted into the LVR-15 reactor, a recirculation pump (RP), which is connected to the test section via the lines 1 and 2 and a compensator (C1), which provides the system with the required pressure of 25 MPa. Except for the pressure tube with its test section, the loop will be located outside the reactor hall. At normal operation, the recirculation pump will provide a mass flow of 0.25 kg/s with a nominal pressure head of 145 m [2]. Two safety systems, also depicted in Figure 1, provide coolant for the fuel element in emergency cases.

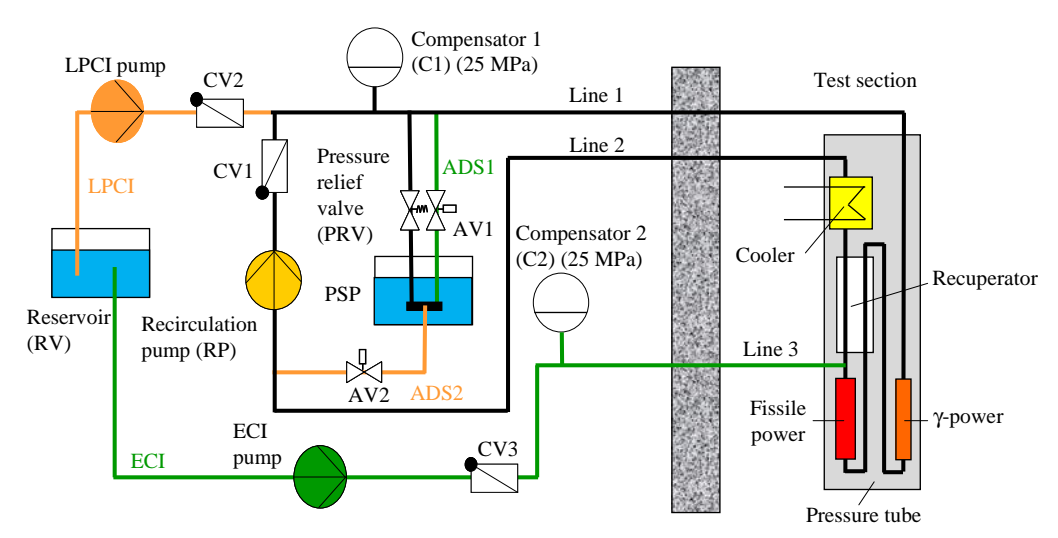


Figure 1 Fuel qualification test loop with safety systems [3].

The low pressure coolant injection (LPCI) is either activated by a drop of system pressure or by low speed of the recirculation pump. In any of these cases, the reactor SCRAM will be activated, the system will be depressurized by the automatic depressurization system 2 (ADS2) and the LPCI pump will run up. At the same time, the recirculation pump will stop and a check valve located downstream will ensure that the coolant will not bypass the test section. Coolant from the compensator will allow a grace period for the LPCI pump to start up, as it provides its coolant inventory to cool the test section passively within the first seconds of this accident.

If we have a closer look at the system, however, we find that this single emergency system will not be capable of handling all types of accidents. In the case of a rupture of line 1, for example, the LPCI pump would feed directly to the break. To deal with such an accident, another independent safety system is needed, which is the emergency coolant injection (ECI), indicated in Figure 1. This system contains another emergency pump, which is supplied by the same reservoir as the LPCI system, and is connected with the test section by an additional emergency cooling line (line 3). This line ends inside the pressure tube, directly above the fuel rods, as visible in Figure 2.

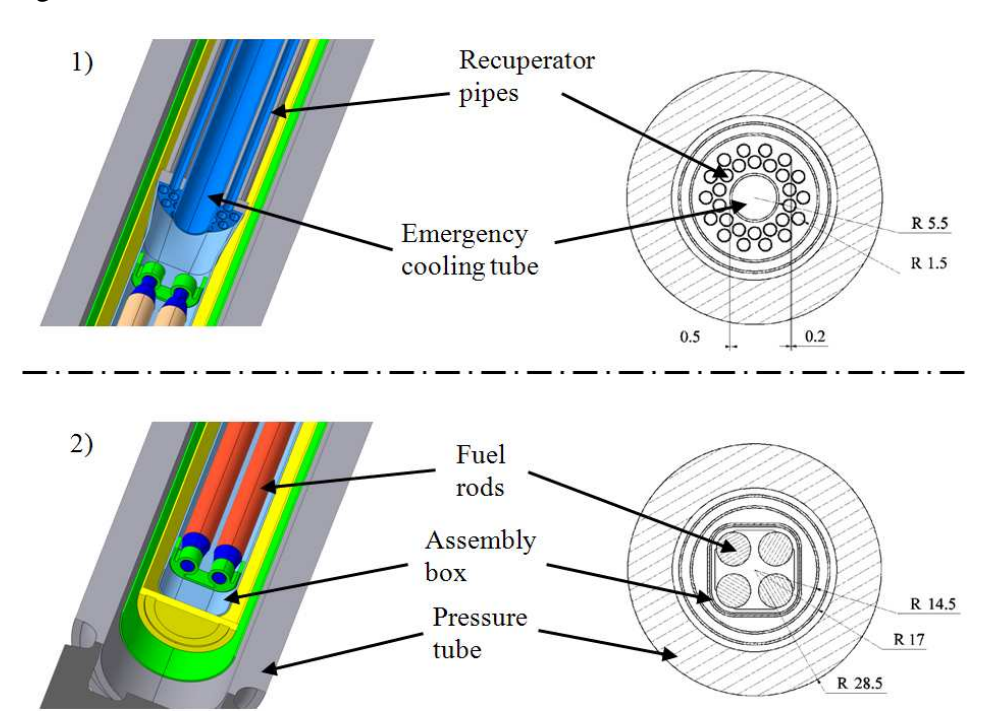


Figure 2 Longitudinal cut through the fuel element. 1) Upper part of the heated section with the transition to the recuperator section. 2) Lower part of the heated section [2].

If this system is activated, the flow direction has to be reversed. Additionally, as in the case above, the reactor SCRAM is activated together with the automatic depressurization system 2 (ADS2). There is also an auxiliary compensator (C2), which feeds coolant to the system, as soon as the system pressure drops. It has to be mentioned that both compensators, as they are completely passive devices, supply their stored coolant regardless where a leakage occurred in

Recirculation pump stops

the system. Both compensators are equal in design and contain 30 liters of water and 24 liters of nitrogen under normal operation, separated by a membrane.

#### 2.1 **Triggers of the emergency systems**

As the position of any break of the coolant lines can hardly be determined automatically, the triggers activating either of the emergency cooling systems can only be based on the available signals as listed in Table 1.

nal	Actions
	Reactor SCRAM

Sign System pressure  $p < p_{min}$ ADS2 opens LPCI pump starts Recirculation pump speed  $n < n_{min}$ Recirculation pump stops System pressure  $p > p_{max}$ PRV opens (spring loaded) Coolant temperature in test section  $T > T_{max}$ : Reactor SCRAM  $T > 500 \, ^{\circ}C$ if p > 22.1 MPa ADS1 opens  $T > T_{sat} + 50 \text{ K}$ if p < 22.1 MPa. ECI pump starts

Table 1: Triggers and actions of the safety systems

As shown in Table 1, the LPCI and the ECI pump are activated by different, independent signals. The temperature signal is dominating the pressure signal in case that both signals are given. The ECI system is always activated by temperature signals, no matter where the break occurred. Either the inlet temperature of the recirculation pump exceeding 350 °C or the temperature surveillance of the heated section might detect the violation of a design limit. These limits are depending on the actual system pressure. For a system pressure greater than 22 MPa, the temperature limit for the coolant in the active zone is 500 °C. For pressures less than 22 MPa, the temperature signal is activated, if the coolant temperature is more than 50 K above the saturation temperature, indicating a dry test section. The performance of this simple system has been assessed by numerical simulations, as will be described below.

#### **3.** Improvements of the APROS model

#### 3.1 Coolant density feedback on the fuel element power

Inlet temperature of main high pressure pump > 350 °C

The Monte Carlo N-Particle Code MCNP5 [5] was used to simulate the neutron flux in the LVR-15 reactor core containing the test fuel element. In these simulations, the core is represented by a box of 80 vertical channels arranged in an 8x10 square lattice with a pitch of 7.15 cm. The box height of 54 cm corresponds to the active length of the fuel element. This simplified reactor core was placed into a water-filled cylinder of 280 cm in diameter and 700 cm height, representing the reactor vessel. Furthermore, the geometry consists of the following components: the fuel assemblies of highly enriched uranium (36wt% <sup>235</sup>U), the control rod assemblies, the neutron reflector, air and water displacement channels and the test fuel element. The model of the reactor core and the test fuel element is depicted in Figure 3.

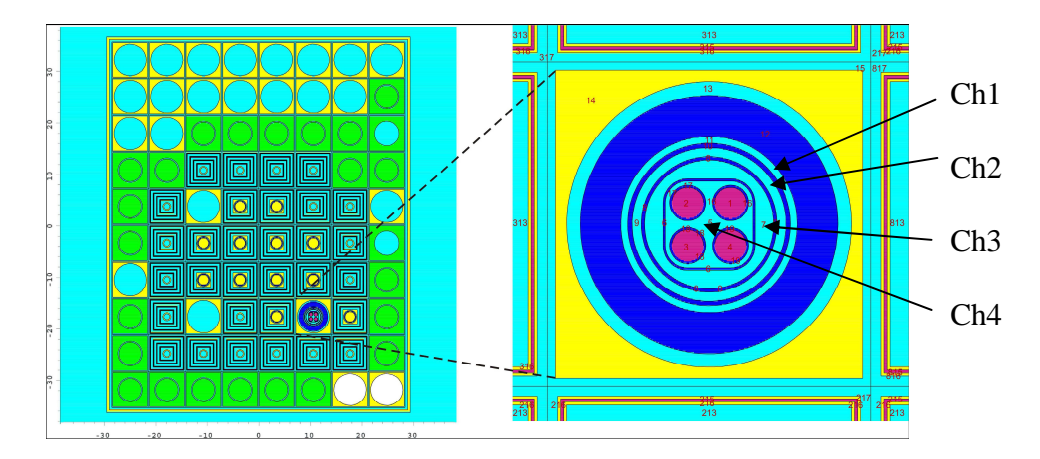


Figure 3 Horizontal cross section of the LVR-15 core as implemented in MCNP5 (left) and details of the active channel (right).

Thus, the calculated axial power profiles gave a symmetric cosine-shaped distribution. For the analysis of the fuel element fissile power, the active length was divided into 14 segments of 4 cm length each. Two different cases were studied in the simulations. The first one called Test Run 1 assumes that the coolant temperature was varied in all four channels of the test fuel element, numbered as 1 to 4 from outside to inside in Fig. 3. In Test Run 2, the variation was done only in the central channel 4, formed by the four fuel pins and the square assembly box around. The latter case was studied to simulate a sudden evaporation of the coolant in the innermost channel. The results of the simulations for different coolant temperatures and densities show that the fuel element power increases with coolant density, as shown in Figure 4.

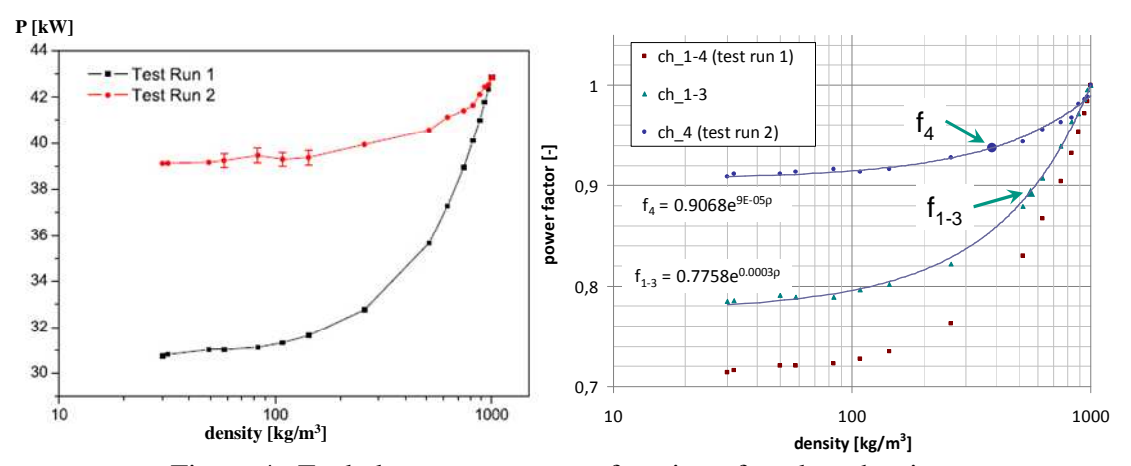


Figure 4 Fuel element power as a function of coolant density.

Moreover, it was found that the coolant temperature inside the pressure tube has very low influence on the value of  $k_{eff}$  and thus on the core reactivity.

To implement the density feedback into the APROS model, the power factor of Fig. 4 was split between a factor  $f_4$  arising from density changes in channel 4 only, and a factor  $f_{1-3}$  arising from the average density change in channels 1 to 3. The latter factor was derived from the results of the Test Runs by dividing  $f_{1-4}$  by  $f_4$ :

$$f_{I-3} = f_{I-4}/f_4. (1)$$

This new curve and the curve for a density change in the inner channel 4 were fitted with exponential functions as shown in Fig. 4. With the average coolant density in the channels 1 to 3 and the average density in channel 4, APROS calculates the factors  $f_4$  and  $f_{1-3}$ . These factors multiplied with the nominal power give the actual fissile fuel element power. For a nominal power of 63.24 kW we obtain the desired fuel element power of 53 kW for steady-state operation, as given in [2].

In addition, 43% of the fissile power is released as gamma radiation. This corresponds to a volumetric heat input of 3 W/g generated in the metal structures of the test fuel element, primarily in the thick walled pressure tube. Thus, under steady state conditions when the fuel element runs at 53 kW fissile power, 76 kW have to be transferred to the cooler in total.

As soon as a reactor SCRAM happens, the fuel element power decreases. After 1 second delay, in which the control rods are released, they need another 3 seconds to fall into the reactor. In this latter period, the power is assumed to decrease linearly with time. For the long term residual heat removal, the rod power is predicted with the decay heat equation (2) [6]:

$$P(t) = 0.0622 P_{Nom} \left( t^{-0.2} - \left( T_0 + t \right)^{-0.2} \right). \tag{2}$$

With  $P_{Nom}$  being the nominal heating power before the SCRAM, t the time elapsed after the SCRAM happened, and  $T_0$  the time that the reactor was running at nominal power before the SCRAM. Here  $T_0$  is assumed to be a very long period to simulate worst case conditions.

# 3.2 Prediction of the cladding temperatures

## 3.2.1 Wall heat transfer

For the six-equation model of APROS, there are three heat transfer zones (zone 1-3) to simulate the different heat transfer regimes [7] for subcritical pressures. Zone 1 is defined as heat transfer in case of a wetted wall. The case of a dry wall, where only the gaseous phase is in contact with the wall, is denoted as zone 3. The transition zone between wetted and dry wall is called zone 2. For the selection of the correct heat transfer zone, the code uses the following parameters: wall temperature  $T_w$ , Leidenfrost temperature  $T_L$ , saturation temperature  $T_{sat}$ , critical heat flux  $q_{crit}$ , wall heat flux  $q_w$ , and void fraction  $\alpha_g$ .

At supercritical pressure conditions, there exist only single-phase convective mechanisms for the heat transfer to the wetted wall, as there will be no boiling. In this case, the homogeneous model would be best but this, in turn, would not lead to a smooth transition to the subcritical state. As it is not possible to change between flow models during depressurization, the contribution of boiling has to be suppressed at supercritical pressures. Furthermore, the formalism of interfacial heat and mass transfer has to be extended artificially to the supercritical pressure regime. Thus, a pseudo-saturation enthalpy and the concept of a pseudo-critical-line are introduced [8]. Here, the fluid is treated as liquid when its enthalpy is below the pseudo-critical enthalpy and as gas when its enthalpy is above the pseudo-critical enthalpy.

A transition zone (zone 2) like in the subcritical state is not needed for supercritical pressures. Furthermore, zone 1 is selected, if the average enthalpy is below the pseudo-evaporation enthalpy; whereas zone 3 is chosen for higher enthalpies. For both zones, the Jackson-Hall correlation [9] is used to predict the heat transfer coefficient, keeping in mind that for deterioration of heat transfer the prediction of the fuel cladding temperatures is not very precise [10]. The correlation is of Dittus-Boelter type and defined as:

$$Nu = 0.0183 \,\text{Re}_b^{0.82} \,\text{Pr}_b^{0.5} \left(\frac{\rho_w}{\rho_b}\right)^{0.3} \left(\frac{\overline{c}_p}{c_{pb}}\right)^n \tag{3}$$

Here, the index b denotes bulk and the index w wall parameters. The exponent n is not constant and depends on the values of  $T_w$  and  $T_b$  in relation to the pseudo-critical temperature  $T_{pc}$ . For our conditions, it ranges between 0.4 and 0.6. The average heat capacity at constant pressure is defined as:

$$\overline{c}_p = \frac{1}{T_w - T_b} \int_{T_b}^{T_w} c_p dT \,. \tag{4}$$

When the system pressure falls to subcritical, it depends on the temperature of the wall, which heat transfer zone is activated. If the wall temperature is greater than the Leidenfrost temperature, zone 3 is active and the heat transfer of the dry wall is determined either as film boiling according to Berenson [11], single phase heat transfer to the gas phase or as natural convection heat transfer, which ever is largest [7]. For wall temperatures between the Leidenfrost temperature and the saturation temperature, zone 2 is used. The heat flux is then interpolated between the critical heat flux q<sub>crit</sub> and the heat flux over the dry wall. Zone 1 is activated as soon as the wall temperature falls below saturation temperature. For this zone, the wall temperature is determined with the heat flux of the wetted wall [7].

There are different correlations implemented in APROS to calculate the critical heat flux in the six-equation model. Here, it is interpolated between the Zuber-Griffith correlation [12] and the Biasi correlation [13] depending on the mass flux. Moreover, the Groeneveld-Stewart correlation [12] is used to calculate the Leidenfrost temperature.

## 3.2.2 Wall friction

For the determination of the single-phase friction factor, there are two models available in APROS; either the smooth tube or the rough tube, whereat in the latter model the wall friction has to be defined for each pipe [7]. For the smooth tube the maximum value of the laminar flow friction and the coefficient calculated with the Blasius correlation [14] is used, whereas the Colebrook equation [15] also considers the roughness of the pipe. In our simulations, APROS automatically uses Colebrook for Reynolds numbers > 4000 and the smooth tube model for smaller Reynolds numbers. For all pipes of our model, a relative roughness of 0.00001 has been used.

At supercritical pressures the wall skin friction factor  $\xi$  for heated walls is calculated with the correlation of Kirillov et al. [16]:

$$\xi = \frac{1}{(1.82\log_{10}(\text{Re}_b) - 1.64)^2} \left(\frac{\rho_w}{\rho_b}\right)^{0.4}.$$
 (5)

Furthermore, a two phase friction multiplier is needed to extend the pressure drop calculation of single phase flow and to estimate the phase distribution on the wall of the flow channel. This multiplier depends on the present flow regime: stratified flow, non-stratified flow without droplet entrainment and non-stratified flow with droplet entrainment. Details are described in [10].

## 3.2.3 <u>Simulation of the heated section in APROS</u>

It has not been possible to simulate the heated section with standard components. Heat exchanger components that are implemented in APROS have only one heat exchanger wall per side. On the contrary, the assembly of the test fuel element is forming co-axial channels, which exchange heat over both walls with their neighbouring channels. For this reason, the heat transfer between the channels is simulated with thermal hydraulic nodes and heat transfer modules. These nodes are thermally connected with their neighbours that are located at the same height in neighbouring channels by three different components.

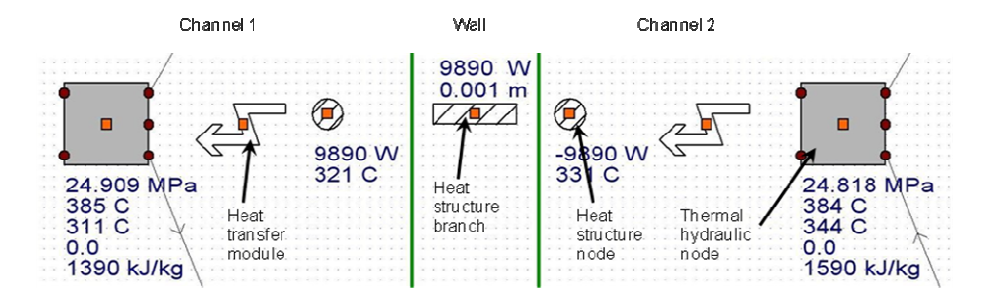


Figure 5 Simulation of two neighboring channels in APROS.

Heat transfer modules are used to calculate the heat transfer coefficient for the respective side of the wall. Heat structure nodes are needed to calculate the wall temperature. A heat structure branch connects two heat structure nodes with each other and calculates the heat flow through the wall with respect to thickness of the wall and its material. Figure 5 illustrates the connection of two thermal hydraulic nodes in two neighbouring channels.

Additional heat input nodes are used to simulate the fission and gamma power input of the four fuel rods. As the heated section is axially divided into four segments, each with a length of 14 cm, the calculated fuel element power is also divided by four for each heat input node. Each of these nodes has an additional heat transfer module, two heat structure nodes and one heat structure branch connected to them to resemble the four fuel rods.

# 4. Simulations of piping failures

In the following, the results of some accident sequence analyses for different kinds of piping failures are presented exemplarily to illustrate the expected performance of the system.

#### 4.1 Break of line 2

As a first example, a break in line 2 is assumed. In this case, the accident will be detected by a low system pressure. This will result in a reactor SCRAM and the activation of the LPCI system. Automatically, both compensators will start to inject their cold, stored water into the system. Thus, the LPCI pump will have up to ~ 50 s time to start and run up for long-term cooling of the fuel rods. It is unlikely that so much time might be needed. The recirculation pump stops simultaneously with the SCRAM. The pressure and temperature progress inside the active zone is illustrated in Figure 6. "Inlet" denotes the inlet into the assembly box at the bottom of the fuel element and "outlet" is the top of the assembly box at the transition to the recuperator. Nodes 1 to 4 are in between.

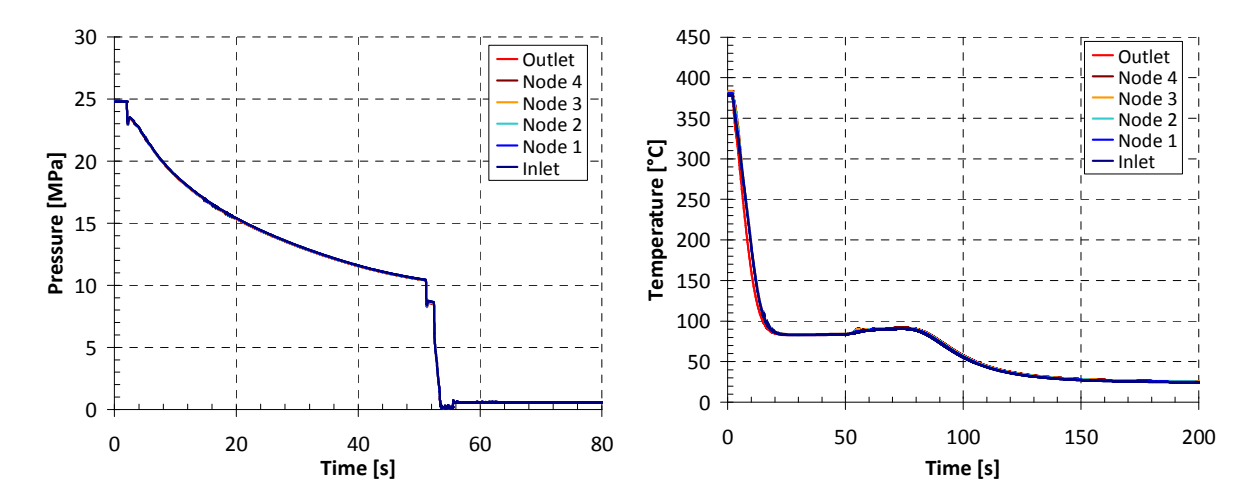


Figure 6 Pressure progress (left) and coolant temperatures (right) of the active section for a break of line 2.

The break of line 2 occurs at time step 2 seconds. As visible, the pressure inside the active zone drops immediately. If the system pressure falls below 12.5 MPa, at the latest, the LPCI pump

must start to inject coolant into the system. Compensator 2 is empty after 51 seconds and compensator 1 is also empty just one second later. Finally, the pressure drops to ambient conditions. The progress of the coolant temperatures show that the fuel rods are well cooled and ambient temperatures are reached after 180 seconds.

## 4.2 Break of line 1 close to the recirculation pump

As a second example, we assume a break in line 1, close to the recirculation pump. As for the accident presented before, the break of line 1 activates the LPCI system as well, even though not being meaningful in this case as the coolant from the LPCI pump does not reach the test section. The analysis of this accident with APROS shows that the system pressure decreases immediately after the break of line 2, which happened again at time step two seconds. It is shown in Figure 7 that the pressure drops to ambient pressure after 18 seconds, when compensator 2 is empty.

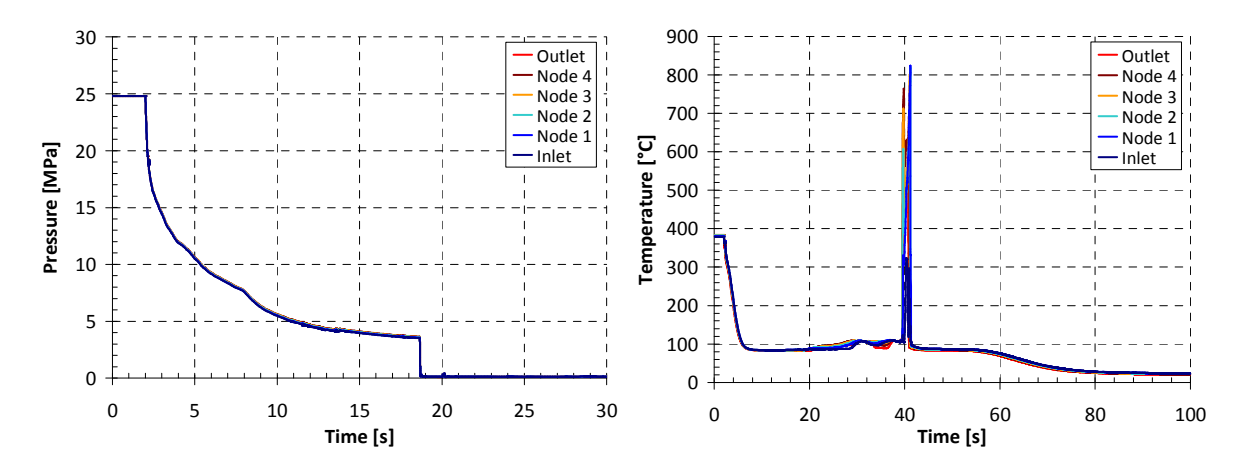


Figure 7 Pressure progress (left) and coolant temperatures (right) of the active section for a break of line 1.

This is an example showing that the safety system does not activate the right system immediately, as the LPCI pump and the compensator 1 feed into the leakage. Moreover, the flow direction through the test fuel element is reversed by the compensator 2. The consequence for the coolant temperatures is shown in Figure 7 on the right. As soon as compensator 2 is empty, there is no more flow through the active zone and the coolant starts boiling. After 38 seconds, the temperature in the active zone is more than 50 K above evaporation temperature and the ECI pump runs up, activated by the temperature signal, and cools the fuel rods again. It can be seen that very high coolant temperatures of more than 800 °C occur after the ECI pump has been activated and before the new coolant reaches the active zone. As the fuel rod power is already very low, however, the cladding temperatures are not much higher and reach 880 °C.

In order to obtain a faster depressurization of the system and to improve the efficiency of the emergency systems, the diameter of the pipe that connects compensator 2 with the loop was decreased. An optimum was found for an inner pipe diameter of 6 mm. Before, all pipes outside the test section had an inner diameter of 14 mm. As illustrated in Figure 8, the depressurization

of the system is accelerated and the cooling period of the test section gets extended due to a smaller mass flow out of the compensator. Now, the coolant temperatures show a small temperature peak at the inlet of the heated section, which is the result of the reduced compensator mass flow and the reversal of the flow direction.

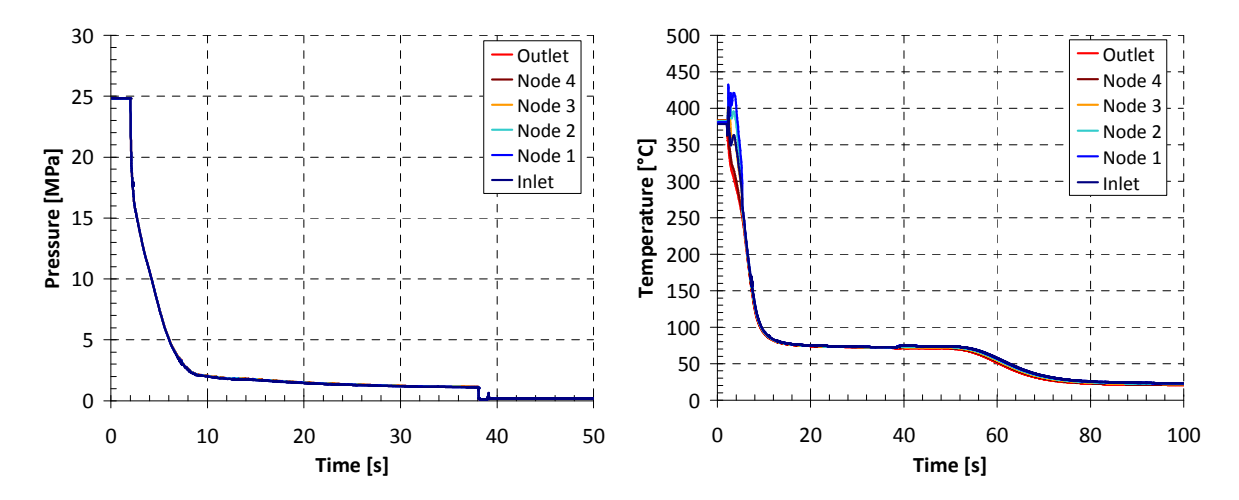


Figure 8 Pressure (left) and coolant temperatures (right) of the active section for a break of line 1 with adjusted compensator piping.

Figure 9 compares the mass flow in the test fuel element for compensator pipe diameters of 14 mm (left) and 6 mm (right). The green curve shows the mass flow out of the emergency cooling line 3. This mass flow is divided into one fraction that leaves the active section immediately through the recuperator (blue curve) and a second fraction that enters the assembly box and cools the fuel rods (red curve).

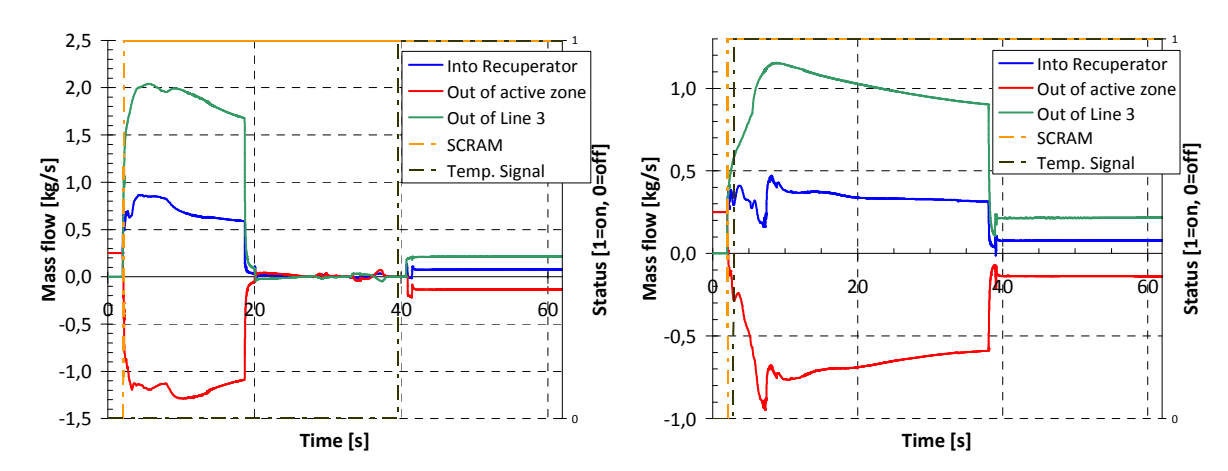


Figure 9 Mass flow in the test fuel element for compensator pipe diameters of 14 mm (left) and 6 mm (right).

It can be seen that the fuel rods are cooled for 38 seconds with the adjusted diameter, which is 19 seconds more than in the case with larger pipe diameter. Furthermore, the mass flow through the

fuel element is never disrupted. This is because the ECI pump gets activated already after 2.8 seconds, as the coolant temperature exceeds the vaporization temperature by more than 50 K, indicated by the temperature peak at the beginning.

## 5. Conclusion and Outlook

The analyses of different accident sequences show so far that the safety systems of the fuel qualification test loop work in principle. Nevertheless, their efficiency can still be improved by the optimization of the trigger signals and piping geometries. Here, the aim is to maintain the coolant mass flow through the test section for any kind of accident and to reach a depressurization in minimum time, in order to avoid critical temperature peaks.

The optimization will be continued as part of the joint European-Chinese project SCWR-FQT with the final objective to design and license the test loop.

# 6. Acknowledgement

This work has been funded by the European Commission as part of their project SCWR-FQT, contract number 269908.

#### 7. References

- [1] T. Schulenberg, J. Starflinger, P. Marsault, D. Bittermann, C. Maraczy, E. Laurien, J. A. Lycklama, H. Anglart, M. Andreani, M. Ruzickova, L. Heikinheimo, "European supercritical water cooled reactor", <u>FISA 2009</u>, Prague, Czech Republic, June 22-24, 2009.
- [2] M. Raqué, A. Wank, T. Schulenberg, P. Hajek, "Thermal analysis of a test fuel element for a reactor with supercritical water", <u>NUTHOS-8</u>, Shanghai, China, October 10-14, 2010.
- [3] R. Schneider, M. Schlagenhaufer, T. Schulenberg, "Conceptual design of the safety system for a SCWR fuel qualification test", <u>NUTHOS-08</u>, Shanghai, China, October 10-14, 2010.
- [4] APROS Version 5.09, VTT Finland and Fortum, http://APROS.vtt.fi/.
- [5] F. Brown, "MCNP a general Monte Carlo n-particle transport code", Version 5. Los Alamos National Laboratory, LA-UR-03-1987, 2003.
- [6] H. Etherington, Ed., "Nuclear Engineering Handbook", p. 7-15, McGraw-Hill Book Company, New York, NY, 1958.
- [7] M. Hänninen, J. Ylijoki, "The constitutive equations of the APROS six-equation model", Manual of APROS Version 5.09, 2007.
- [8] J. Kurki, "Simulation of thermal hydraulic at supercritical pressures with APROS", IYNC 2008, Interlaken, Switzerland, September 20-26, 2008.
- [9] J.D. Jackson, W.B Hall, "Forced convection heat transfer to fluids at supercritical pressure", *Turbulent Forced Convection in Channels and Bundles*, Vol. 2, pp. 563-611, Hemisphere, New York, 1979.
- [10] M. Hänninen, J. Kurki, "Simulation of flows at supercritical pressures with a two-fluid

- code", NUTHOS-7, Seoul, Korea, October 5-9, 2008.
- [11] P.J. Berenson, Film-Boiling Heat Transfer From a Horizontal Surface, Journal of Heat Transfer, August 1961, p. 351-358.
- [12] D.C. Groeneveld, C.W. Snoek, "A comprehensive examination of heat transfer correlations suitable for reactor safety analysis", *Multiphase Science and Technology*, Vol. 2, pp. 181-274, 1986.
- [13] I. Kokkonen, "Air/water countercurrent flow limitation experiments with full-scale fuel bundle structures", *Experimental Thermal and Fluid Science*, Vol. 3, Issue 6, pp. 581-587, 1990.
- [14] H. Oertel jr, M. Böhle, "Strömungsmechanik", Vieweg, Braunschweig / Wiesbaden, 2002.
- [15] N.I. Kolev, "Multiphase Flow Dynamics 2, Thermal and Mechanical Interactions", Springer-Verlag, Berlin, 2002.
- [16] I. Pioro, R. Duffey, T. Dumouchel, "Hydraulic resistance of fluid flowing in channels at supercritical pressures (survey)", *Nuclear Engineering and Design*, 231, pp. 187-197, 2004.